

Accuracy issues in comparisons of time- and frequency-domain polarization mode dispersion measurements

P.A. Williams

*Optoelectronics Division - National Institute of Standards and Technology
325 Broadway, Boulder CO 80303, U.S.A.*

If experimental comparisons are to be made between time- and frequency-domain measurements of polarization mode dispersion PMD, they must be done with a good understanding of the systematic and random uncertainties present. In this paper, I quantify sources of systematic uncertainties in time domain PMD measurements and demonstrate correction techniques on experimental data.

Until recently, theoretical and experimental work [1-10] claimed to support an equality between PMD measured in the time domain as the square root of the second moment σ of the autocorrelation function and PMD measured in the frequency domain as the RMS differential group delay (DGD), so that RMS DGD/ $\sigma = 1$. However, the recent theory of Heffner [11] shows the issue to be more complicated, with RMS DGD/ σ depending on the spectral shape of the time domain measurement source and only for large values of PMD-bandwidth product does the ratio demonstrate a constant value 0.866 which disagrees with previous theory by about 13%. Most of the referenced attempts to measure the RMS DGD/ σ ratio lacked the precision to see a 13% effect. Furthermore, standard second moment evaluations of time-domain PMD have several sources of systematic uncertainties large enough to nullify comparison efforts. These systematic errors were avoided by one recent experimental work [12] which used a curve-fitting method to measure σ giving a value of RMS DGD/ σ close to 0.9. However, curve-fitting is not always considered to be rigorous enough. So, I present corrections here which allow significant reductions of the systematic biases of the standard second moment calculation.

Measurements of PMD in highly polarization-mode-coupled optical fibers using an interferometric or equivalently wavelength scanning with Fourier transform (WSFT) technique produce an autocorrelation function illustrated by the one-sided example of Figure 1. This time domain response is a quasi-random amplitude (due to random phasing) under a Gaussian envelope. The PMD of the fiber can be measured by finding the square root of the second moment of this curve [13,14]

$$\sigma = \sqrt{\frac{\int I(t) t^2 dt}{\int I(t) dt}} \quad (1)$$

However, in calculating this quantity, systematic errors due to numerical integration, data clipping and central peak removal are encountered and must be corrected.

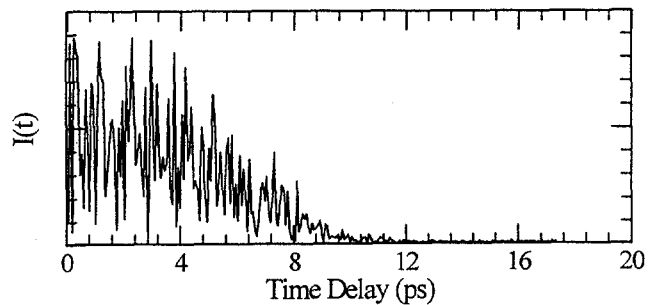


Figure 1 Typical Fourier-transformed wavelength scanning data.

A good approximation to Equation (1) is obtained using the trapezoidal integral approximation

$$\sigma = \sqrt{\frac{\sum_{k=a}^b I(t_k) t_k^2 - \frac{1}{2} I(t_a) t_a^2 - \frac{1}{2} I(t_b) t_b^2}{\sum_{k=a}^b I(t_k) - \frac{1}{2} I(t_a) - \frac{1}{2} I(t_b)}} \quad (2)$$

where t_a and t_b are the time coordinates of the first and last points used. A simpler rectangular approximation is sometimes used [13,14]. However, the numerical integration is usually carried out with the time coordinate sampled at the practical values $t = 0, \Delta, 2\Delta, \dots$ for example, as opposed to the more appropriate $t = \Delta/2, 3\Delta/2, 5\Delta/2, \dots$ values (Δ is the sampling step size). It should be cautioned that for a single-sided data set as from WSFT, integrating from $t_a=0$ will underestimate σ by an amount dependent on the time domain sampling density η (number of data samples / σ). Under practical conditions, this can result in errors of several percent and the trapezoidal approximation represents a significant improvement (Figure 2).

Another systematic bias comes from limited range. The sampling range t_b can be limited by the wavelength resolution in WSFT measurements or the scan range of the interferometer. But, the first limit to be encountered is likely to be due to the signal to noise ratio of the system. Generally, the useable portion of the data is determined by some criteria such as the exclusion of data beyond the point t_b where the signal drops below 2 times the rms noise level [13,14]. However, clipping the data wing(s) in this way systematically biases the measured σ toward lower values. This can be seen from Equation (1) in that for a nominal gaussian, at large values of t , the positive integrand of the denominator $I(t)$ approaches zero more quickly than the positive integrand of the numerator $I(t)t^2$. So, the result of excluding data at large values of t will be to bias σ toward smaller values. Figure 3 shows a computer simulated result of measurement error as a function of the data clipping point t_b/σ (solid curve) with σ being the true value of the square root of the second moment. The clipping error is substantial. Indeed, an RMS noise level of 6 or 7% would require clipping at $t_b/\sigma = 2$ giving an error on the order of 10% – large enough to bias measurements of RMS DGD/ σ from 0.866 up to 1.0.

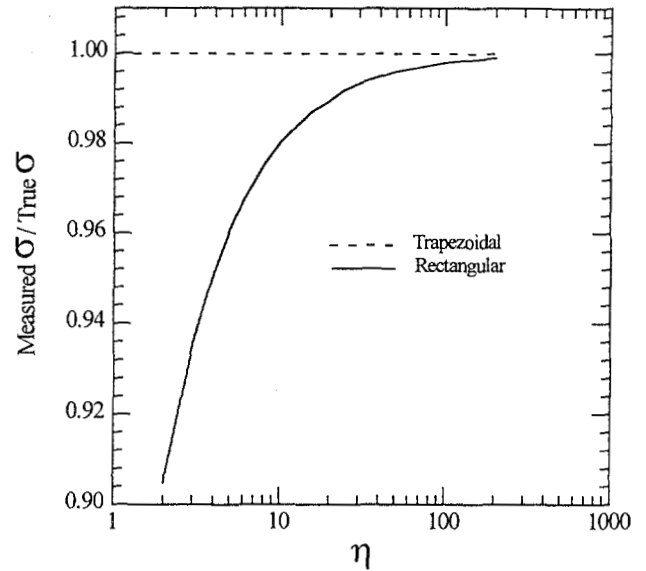


Figure 2 Measurement errors for trapezoidal (dashed) and rectangular (solid) integral approximations as a function of sampling density (the number of sampled points/ σ) η .

To correct for this error, a simple look-up table is useful. The dashed curve of Figure 3 is the solid curve plotted as a function of t_b/σ_M where σ_M is the measured value of second moment. In practice, dividing σ_M by the value of the dashed correction curve at t_b/σ_M removes the clipping error. Of course, the correction has trouble for values of t_b/σ_M which are much less than 2 where the curve becomes very steep and small random errors in measuring σ_M are amplified by the correction factor. An example of the correction performance is shown in Figure 4 where σ is measured on simulated WSFT data (using the simulation of Reference 11) at various clipping levels and then compensated to give a corrected value. Clearly, the compensated σ performs well, within 2% of its unclipped value down to about the $t_b/\sigma_M = 2$ level.

Another source of systematic error comes from removing the central peak from the time domain response. In autocorrelation interferometers, the interferogram has a large source autocorrelation peak around $t = 0$ which contains no PMD information. A similar peak results from windowing in WSFT. In practice, σ is often calculated by simply adjusting t_a in Equation 2 to skip the data points under the central peak. However, the result is a systematic increase in measured σ . The reason can be seen in Equation 2, where eliminating low t values of $I(t)$ reduces the value of the denominator more drastically than does eliminating low t values of $I(t)t^2$ from the numerator. The simplest technique to compensate this error is to substitute the values of $I(t)$ where the central peak occurs with estimates of what $I(t)$ would be without the central peak. As an example, this is illustrated for single-sided WSFT data (the procedure is identical for interferometric data). First, σ_M is measured using Equation (2) with t_a set to ignore values of $I(t)$ which are dominated by the central peak. Then σ_M is used to define new integration limits $t_a = \sigma_M/2$ and $t_b = \sigma_M$. Then $\sigma_{0.5-1}$ is measured using Equation (2) with these new limits and divided by 0.75 (the value of $\sigma_{0.5-1}$ for an ideal Gaussian of unit amplitude). The result of this division is an estimate at the amplitude A of the Gaussian

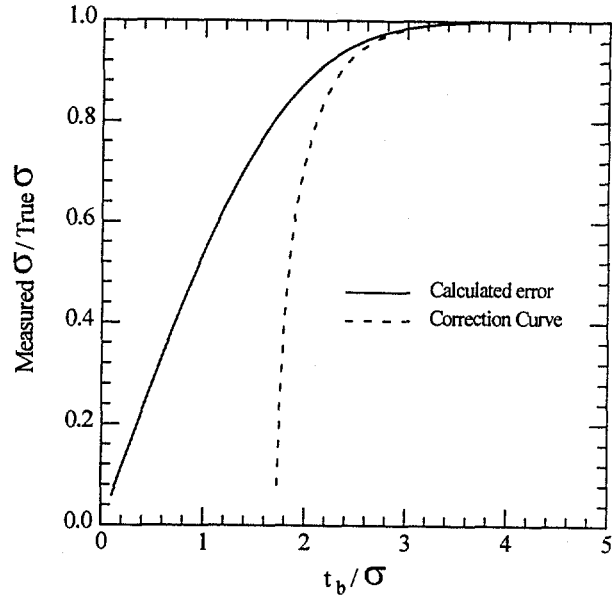


Figure 3 Data clipping error vs. sampled fraction of true second moment (solid) or measured second moment (dashed).

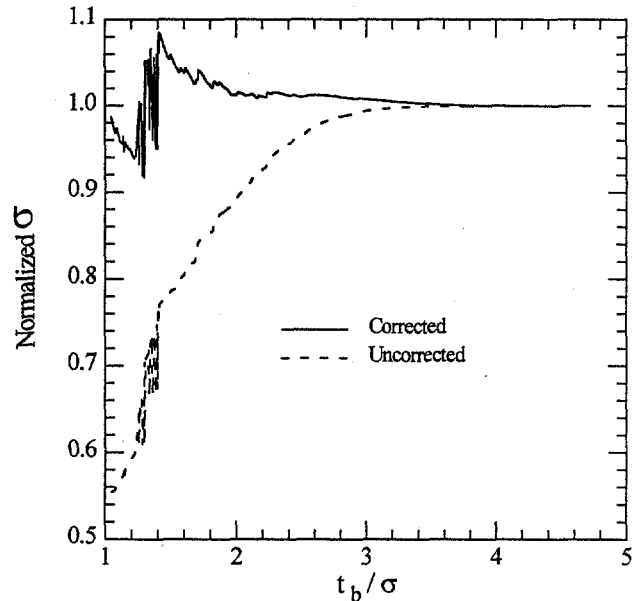


Figure 4 Normalized simulated measurements of uncorrected (solid) and corrected (dashed) second moment vs. sampled fraction of second moment.

function describing the time-domain response

$$I(t) = A \exp\left(\frac{-t^2}{2\sigma^2}\right). \quad (3)$$

Then, σ_M and A are used along with Equation (3) to generate estimated values of $I(t < t_a)$. Finally, σ is recalculated using equation (2) with $t_a=0$. An example of the error and correction results is shown in figure 5 for computer simulated interferometric data.

It is worth mentioning that there is one systematic error in time domain measurements which is well known but often inappropriately corrected for. I refer to the source width subtraction technique

$$\sigma_{True}^2 = \sigma_{Meas}^2 - \sigma_{Source}^2. \quad (4)$$

The idea is to subtract the square root of second moment of the Fourier transform of the optical source spectrum σ_{Source} from the measured square root of the second moment of the interferogram σ_{Meas} to yield the true square root of the second moment of the spectral response of the device under test σ_{True} . This technique comes from the fact that a function which is the product of two other functions has a variance of its Fourier transform which is equal to the sum of the variances of the Fourier transforms of the other two functions. However, application of Equation (4) to a WSFT or interferometric PMD measurement is inappropriate since σ_{Meas} is measured after the time domain response has undergone a non-linear enveloping technique. Specifically, this involves using the envelope of the photocurrent in the interferometric case or using the magnitude of the Fourier transform in the WSFT case. Both of these enveloping functions are non-linear modifications to the process which make Equation (4) non-applicable. So, while a finite source width still contributes a systematic bias to the measured second moment, there is not yet a rigorous method of correcting the error.

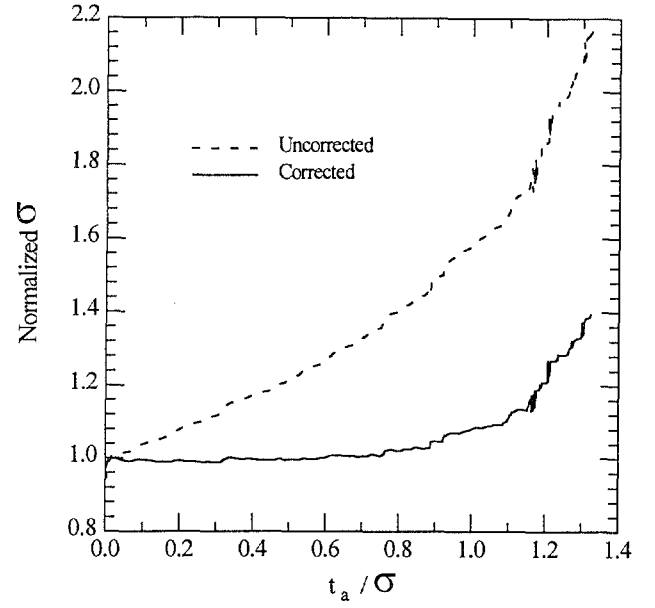


Figure 5 Normalized simulated measurements of uncorrected (solid) and corrected (dashed) second moment vs. starting measurement time/measured second moment.

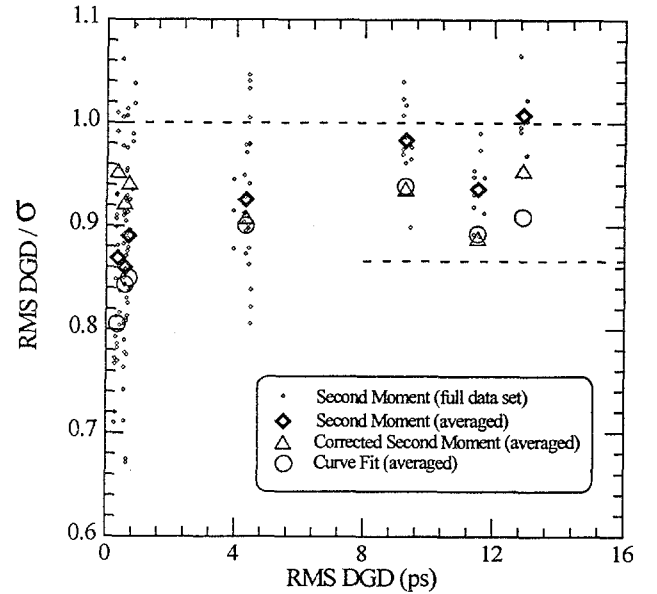


Figure 6 Ratio of frequency- and time-domain PMD measurements as a function of PMD.

In order to demonstrate the usefulness of the above corrections, the value of $\text{RMS DGD}/\sigma$ is calculated using the data set from reference [12]. The data represents measurements of seven different fiber specimens using both Jones matrix eigenanalysis and WSFT techniques. σ is extracted from the WSFT data using Equation 2 with no correction factors. Then, the same σ is corrected using the above techniques. Finally, a third set of second moment values are obtained by performing a non-linear least squares fit of Equation 3 to the data sets. This curve-fit technique is not as susceptible to the systematic errors described above and acts as an estimate of the true value of σ . In Figure 6, the ratio of the frequency domain measurement of PMD (RMS DGD) and the associated time domain measurement σ are plotted as a function of the PMD of the fiber (RMS DGD). The upper dashed line indicates the previously predicted 1.0 ratio and the lower dashed line illustrates the asymptotic 0.866 value predicted by Heffner. The large data points represent the average of several statistically independent measurements. The small diamonds are the unaveraged uncorrected second moment measurements to illustrate the spread in data and the number of measurements. Clearly, the uncorrected second moment data yields values with a systematic bias of $\sim 5\%$ above the curve fit results. Application of the correction techniques to the data brings the second moment values into good agreement with the curve fit results as expected. Clearly, the corrected results indicate a ratio which is closer to 0.866 than to 1.0. However, a larger population of measurements is needed to make a quantitative judgement.

My thanks go to B.Heffner for providing some of the simulated data used in this work and for sharing with me some insight into the world of PMD.

- [1] N.Gisin, Opt. Commun., **86**, 371-373 (1991).
- [2] N.Gisin, and J.P.Pelloux, Optics Communications, **89**, 316-323 (1992).
- [3] B.Perny, C.Zimmer, F.Prieto, and N.Gisin, Electron. Lett., **32**, 680-681 (1996).
- [4] M.Artiglia, A.Chiantore, and A.Rossaro, Proc. Optical Fiber Measurements Conference '95, p. I.4 (1995).
- [5] M.Artiglia, P.Morra, and C.Sartori, Proc. Optical Fiber Measurements Conference '95, p. II.6 (1995).
- [6] N.Gisin, Proc. Symp. Optical Fiber Meas. '94, 149-154 (1994).
- [7] N.Gisin, R.Passy, J.C.Bishoff, and B.Perny., IEEE Phot. Tech. Lett., **5**, 819-821 (1993).
- [8] Y.Namihira and J.Maeda, Elec. Lett., **28**, 2265-2266 (1992).
- [9] Y.Namihira and J. Maeda, Proc. Symp. Optical Fiber Meas. '92, 145-150 (1992)
- [10] N.Gisin, R.Passy, B.Perny, A.Galtarossa, C.Someda, F.Bergamin, M.Schiano, and F.Matera, Electron. Lett., **27**, 2292-2293 (1991).
- [11] B.L.Heffner, Opt. Lett., 113-115 (1996)
- [12] P.A.Williams and P.R.Hernday, Proc. Opt. Fiber Meas. Conference '95, p. I.2 (1995).
- [13] Fiber Optic Test Procedure (FOTP) 113, Telecommunications Industry Association.
- [14] Fiber Optic Test Procedure (FOTP) 124, Telecommunications Industry Association.